Finite Element Modeling of Gyroid Structures Subjected to Impact Loadings

Ramos, H. [1], Santiago, R. [1], Alves, M. [2], Theobald, P. [3], Soe, S. [3] Brasil, R. [1]

[1] Centre of Engineering, Modelling and Applied Social Science (CECS), Federal University of ABC (UFABC) / Brazil.

[2] Department of Mechatronics and Mechanical Systems Engineering, Group of Solid Mechanics and Structural Impact, University of São Paulo (USP) /Brazil.

[3] Cardiff School of Engineering Cardiff University / UK.

The gyroid based structure is a type of triply periodic minimal surface (TPMS), which nowadays can be realized by additive manufacturing techniques. This is a promising lightweight structure, that can be of great use in mitigating impact energy, when gyroid structures are used as kinetic energy absorbers. In this paper, a gyroid structure stands modeled via the finite element method. The gyroid is subjected to the impact of a dropping mass. The material was subjected to an extensive characterization based on digital image correlation. Johnson-Cook material parameters were obtained. The FE models were evaluated by comparing the force-displacement response to experimental impact tests. The FE models were able to represent the overall response of the gyroid under a different level of impact loadings.
Keywords: Gyroid, Finite Element, Additive Manufacturing, Impact Resistance, Lattice Structure

INTRODUCTION

The advent of additive manufacturing (AM) allowed the production of complex geometries such as gyroids, trusses, and other lattices structures, which are barely possible using traditional manufacturing processes (such as, subtractive manufacturing). AM is able to manufacture complex three-dimensional objects directly from computer-aided design models (Qiu et al, 2013), allowing various mechanical properties to be placed selectively within a structure and enabling complex multi-part design interactions to be rapidly fabricated with trivial effort. Complementary, these structures have shown promising application as impact absorbers and lightweight elements.

Direct metal laser sintering (DMLS) is an AM technique using a powder-bed fusion process to manufacture near fully dense metal components with complex geometries. Selective laser melting (SLM) is a DMLS which melts successive layers of metal powder (Gorny et al, 2011), such as stainless steel (McKnown et al, 2008, Yan et al, 2012), titanium alloy (Gorny et al, 2011, Mullen et al, 2009, Murr et al, 2010) and copper (Ramirez et al, 2011).

McKnown et al. (2008) manufactured 316L stainless steel lattice structures based on two types of unit cells by SLM, exploring its compression and blast loading response, the lattice structures were based on [±45°] and [0°, ±45°], unit-cell topologies. During the compression tests, a buckling mode of failure was observed in the lattice structures, whereas a stable progressive collapse was evident in the structure. The blast resistance of the lattice structures increased with increasing yield stress. Yan et al. (2012), studied the evolution of manufacturability and performance of SLM produced periodic cellular lattice structures made with stainless steel. In his conclusion, he proves which yield strength and Young's modulus of the gyroid cellular lattice structures increase with the decrease in the unit cell size due to the denser struts of the lattice structures with smaller unit cell sizes.

Gorny et al. (2011) explored titanium on SLM-processed as well as heat treated lattice structures made from Ti6Al4V alloy that were employed for mechanical testing. It is demonstrated that the current approach provides means to understand the microstructure-mechanical property/local deformation relationship to allow for optimization of load adapted lattice structures. Mullen et al. (2009), studied titanium cellular structures through SLM for bone in-growth applications. These cellular structures could provide porosity and compression strength comparable to the typical behavior of natural bones. Murr et al. (2010), used Ti6Al4V open cellular foams fabricated by additive manufacturing using electron beam melting (EBM). These foams exhibit the potential for novel biomedical, aeronautics, and automotive applications.

Ramirez et al. (2011), fabricated a reticulated mesh and stochastic open cellular foams using copper, fabricated by additive manufacturing using electron beam melting with densities ranged from 0.73 g/cm3 to 6.67 g/cm3. These open cellular structure components exhibit considerable potential for novel, complex, multi-functional electrical and thermal management systems, especially complex, monolithic heat exchange devices.

The use of aluminum alloys in SLM has some limitations due to its poor flowability (Yan et al, 2015), high laser reflectively, thermal conductivity and oxidation (Thijs et al, 2011, Ameli et al., 2013). Recently, Ameli et al. (2013), used SLM for manufacturing aluminum heat pipes with porous wick structures designed by repeating an octahedral unit cell. It showed that the SLM was able to manufacture complex aluminum designs with different thickness, porosity, permeability and pore sizes.

Besides the challenges of using SLM for manufacturing aluminum alloy structures, only a few studies have focused on modeling AM lattice structures by using the finite element (FE) approach. Abueidda et al (2017), developed three types of TPMS using a novel polymeric cellular material manufactured by the SLS process. The TPMS were investigated using an experimental and numerical approach, achieving higher stiffness and strength than other lightweight materials. The gyroid structure is a closed-cell TPMS, which can be used to create multi-functional structures. The gyroid is a smooth and continuous surface, infinitely extended, which divides the space into two congruent inter-twined regions. Additionally, the gyroid presents a zero-mean curvature (Maskery et al, 2017) that might contribute to promoting its energy absorption performance. This warrants further investigation.

Many cellular materials are cellular solids founded on natural materials like wood, fruits, bones, and coral. All support large static, dynamic, and cyclic loads over a long period of time. The structural use of natural cellular materials by man is as old as history itself. The architecture of cellular materials can be designed and optimized to create materials with multifunctional properties including high stiffness, strength, energy absorption, and damage tolerance, among others (Xiong et al, 2015) (Valdevit et al, 2011) (Shaedler et al.,2016).

The TPMS gyroid was discovered by Shoen, A. (1970), where he described an infinitely connected, bi-continuos closed-celled triply periodical minimal surfaces. TPMS are promising porous structures which can be used to create multifunctional material for various applications. They are smooth, infinitely extending continuous surfaces that divide the space into two congruent intertwined regions. Additionally, the average curvatures at each point on the TPMS are null, it means that TPMS possess a zero-mean curvature (Maskery et al,2017).

A periodic surface like a honeycomb lattice consists of an arrangement of hexagons doubly periodic, with the lattice described by two vectors, v and w. With a single hexagon, the vectors enable generation of a large lattice. The gyroid has a similar structure. It is triply periodic, meaning that a small piece of the surface can be used to assemble the entire lattice, by taking a fundamental piece and translating and rotating copies in three independents directions in space.

Scherer, M. R. J. (2013) describe a single gyroid of constant means curvature can be approximated by a level surface. Although this approach does not result in a constant means curvature surfaces, it is extremely useful for simulation.

Consisting of a TPMS in a body-centered cubic (bcc) lattice, the gyroid the approximated by isosurface of the equation (1),

$$g(r) = \sin\left(\frac{x}{a}\right)\cos\left(\frac{y}{a}\right) + \sin\left(\frac{y}{a}\right)\cos\left(\frac{z}{a}\right) + \sin\left(\frac{z}{a}\right)\cos\left(\frac{y}{a}\right) = 0 \qquad (1)$$

where a is the lattice constant (Von Schnering et al, 1991) (Grin et al 2011).

MATERIAL AND METHODS

Material and Manufacturing

The gyroid structures, Fig, 1, studied here were made by commercial aluminum powder Renishaw AlSi10Mg-0403, processed in a Renishaw SLM machine, with 25µm layer thickness and 200W laser.
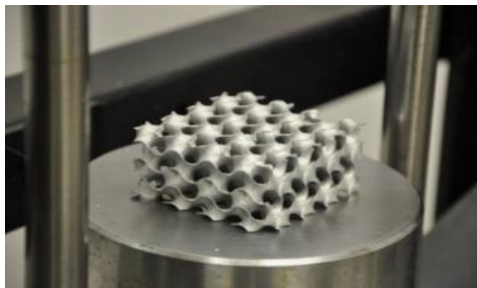

Figure 1 – (a) Gyroid lattice structure

Experimental Analysis

Tensile specimens were manufactured following the same procedure described above, to enable characterization of the material response, Fig. 2b. Uniaxial tensile tests were conducted using an Instron 3369 universal machine at quasistatic strain rate, Fig. 2b.

During the tests, the three-directional deformation of a speckle pattern painted on the sample surface was recorded by two high-resolution cameras, see Fig 2b, covering the specimen width and thickness. For this, a high contrast black-white speckle pattern was applied on the specimen surface. Specimen deformation was measured by a digital image correlation (DIC) system made by Correlated Solutions. Digital image correlation (DIC) analysis of the recorded images gave the true strains at the specimen surface. This technique is able to measure the full-field material strain, synchronized with the testing rig and up to high strain levels.

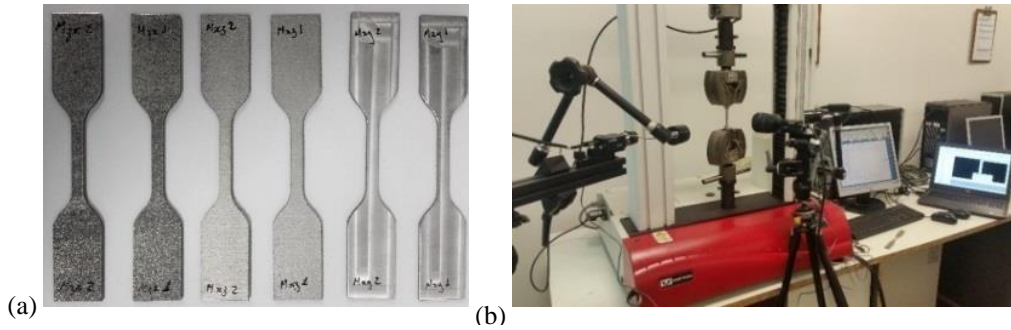(a)   (b)

Figure 2 – (a) Gyroid lattice structure with a relative density of 15.16% and (b) tensile test specimens manufactured by SLM process. (c) Mechanical characterization test using DIC.

For this purpose, a subset grid was defined on the specimen surface, see Fig.3, from where the DIC can extract the complete full-field strain evaluation. The material current stress σ_c, was obtained by adjusting effective specimen cross section using the transverse ε_2 and trough thickness strain ε_3, as

$$\sigma_c = \frac{F_1}{tw(1+\varepsilon_2)(1+\varepsilon_3)},$$
(2)

being the specimen thickness and width represented by t and w respectively, with strain ε_2 and ε_3 obtained from DIC. The strain was measured using an incremental procedure taken from regions close to the material rupture (Lagrangian approach).
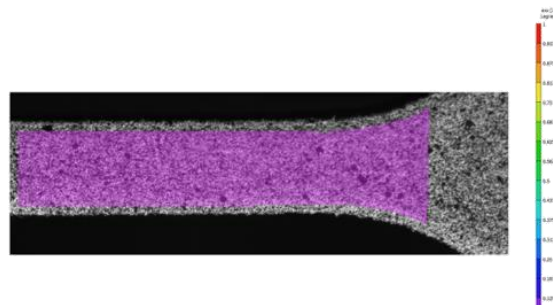

Figure 3 – Shows the DIC plastic strain in the center of the neck for gyroid samples impact tests.
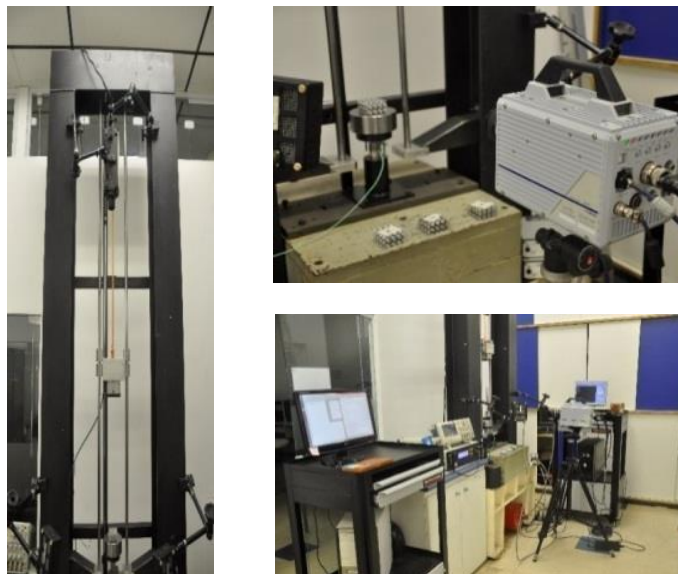

Figure 4 – Drop hammer testing rig set-up for gyroid samples impact tests.

Impact Analysis

The gyroid structures were subjected to impact loading by using a drop hammer rig, Fig. 4, at impact conditions of 10 Kg / 2 ms^{-1} and 10 Kg / 4 ms^{-1}. The impact event was monitored by a laser vibrometer Polytec OFV 3020 and a Kistler 9341B load cell, providing velocity and load data at 10,000 samples/s. A Photron SA-5 high-speed camera was also used, providing impact images at the rate of 3,000 FPS.

In drop hammer tests, a mass is lifted to a certain height and then released, to cause an impact upon a gyroid structure placed at the base of the rig. The free fall maximum velocity achievable is governed by the total height of the drop hammer. These test methods simulate real impact events, such as the automotive crash.

MATERIAL BEHAVIOUR EXTRACTION

Finite element model

The numerical analysis was performed using the Abaqus/Explicit commercial code, modeling gyroid 4x4x4 cells developed in Matlab and implemented on Autodesk Inventor CAD3D software, Fig. 5b. The FE model uses shell elements (C3D8), clamped on the bottom surface and impacted by the discrete rigid flat surface, with the same mass/velocity conditions used on experimental tests. A mesh sensitivity analysis was performed, with an element size of 0.39 mm size presenting the most efficient combination of processing time and numerical accuracy. Fig. 6a, shows the tensile test specimen on the FE model.
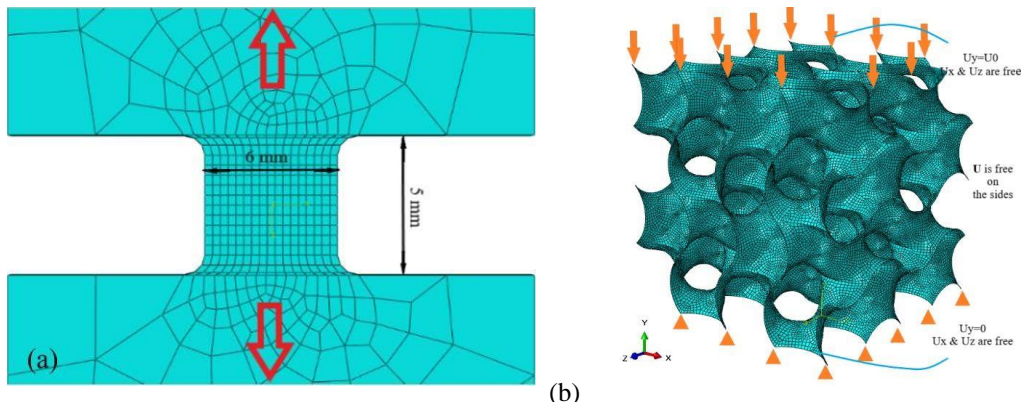

Figure 5 –(a) Tensile test specimen FE model and (b) example of FE mesh and boundary conditions of gyroid structures

The aluminum AM material was modeled using the Johnson-Cook (JC) constitutive model (Johnson R, 1983), Eq. 2, which considers material plasticity, damage, and failure. In this, the plastic deformation σ_p is defined by the elastic and plastic strain as $\varepsilon = \varepsilon_p - \varepsilon_{elastic}$, in an exponential constitutive relationship defined by parameters A, B, and n. Strain rate, temperature and damage effects were neglected at this stage.

$$\sigma_p = \left[A + B\left(\varepsilon_p\right)^n\right] \tag{2}$$

Material behavior for AISI10Mg-0403

The local strain, stress and strain rate are calculated and evaluated by combining the experimental and simulated results. The experiments provide the global stress-strain behavior of the specimen, whilst the simulations give the relations between force and local stress and between displacement and local strain in the stress concentration area of the specimen in the function of the specimen elongation. This relation is highly dependent on the material behavior, geometry, and thus on the material model parameters used in the FEA model. The JC parameters were initially extracted from experimental data, which were then modified by comparing the material strain-stress response obtained from experimental and from the FE model of the uniaxial tensile specimen, Fig.6. The parameters used are presented in Table 1. The Fig. 6 shows the local effective Cauchy Stress versus Lagrangian Strain curve extracted from experimental results and comparison obtained from the FE model. The strain hardening and maximum strain presented on the corresponds curves is highly compatible.

Table 1 – Johnson-Cook constitutive parameters for aluminum alloy Renishaw AISI10Mg-0403.

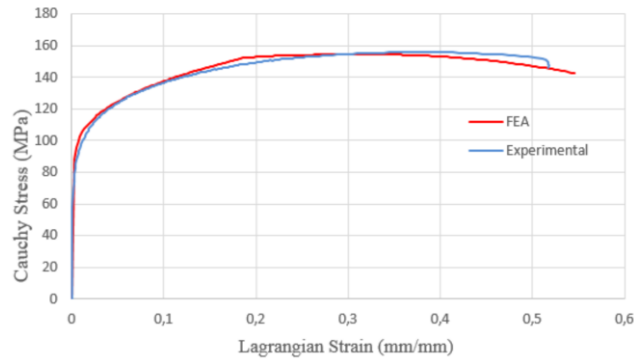| A(MPa)	B(MPa)	n
73.727	122	0.3

Figure 6 – Comparison of the material strain-stress response obtained from experiment and FE model.

RESULTS AND DISCUSSION

Evaluation of the gyroid behavior and the corresponding material model is done by comparing the simulated and experimental stress-strain curve. The qualitative comparison between the FE model and experiment revealed a strong agreement with Fig. 7.

It was noted that the force-displacement response of the gyroid structure clearly presents a plateau region in which the structure collapses and deforms plastically. It was also observed that the structure presents an initial crush-band stage and a residual spring-back after impact. Fig.7 presents a sequence of images of the gyroid deformation during the impact event.
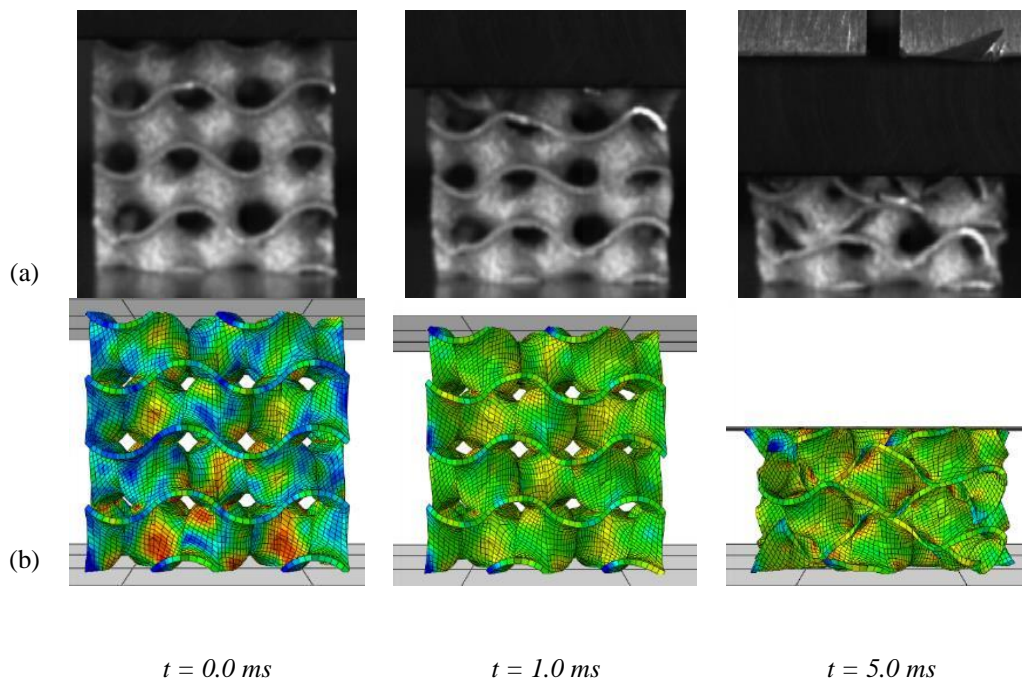

(a)

(b)

t = 0.0 ms   *t = 1.0 ms*   *t = 5.0 ms*

Figure 7 – Qualitative comparison of gyroid response during (a) experimental impact test and (b) FE model.

Additionally, the comparison between the force-displacement responses of the gyroid samples were obtained experimentally and from FE models, Fig. 8. It is shown that the FE could predict the overall response of the sample for both impact conditions studied. The initial accommodation stage of the structure was not predicted by the FE model, presenting scope for further investigation.
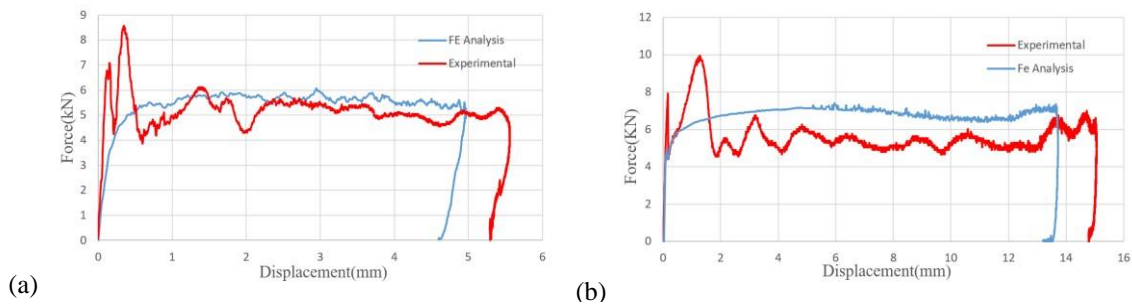
(a)　　　　　　　　　　　　　　　　　　　　　　　(b)

Figure 8– Comparison between experimental impact (red) and FE analysis (blue) (a) at 14.8 Kg / 2ms^{-1} and (b) 14.8 Kg / 4ms^{-1}.

CONCLUSIONS

This study evaluates the manufacturing and performance of periodic cellular lattice structures by a finite element model. Experiments show that the strain hardening of the aluminum power is highly compatible with plastic deformation in a tensile experiment. The Johnson-Cook model was used in the FEA to model the material behavior. The parameters of that model were deduced from the experimental results by use of the simulated strain distribution itself.

The mechanical response of gyroid structures fabricated from SLM aluminum alloy was numerically modeled, designed by repeating a unit cell type which possesses circular structures and a spherical core. The FE model constitutive parameters were extracted from experimental mechanical characterization experiments, enabling characterization of the strain-stress response up to the non-linear plastic regime. An FE model of the gyroid was developed and able to predict the overall qualitative and quantitative response, when subject to different impact loadings.

Further developments of this research are focused on enhancing the FE results, implementing strain-rate, damage and experimental rig inertia

ACKNOWLEDGMENTS

REFERENCES

Ameli, M., Agnew, B., Leung, P.S., Ng, B., Sutcliffe, C.J., Singh, J. and McGlen, R., 2013. "A novel method for manufacturing sintered aluminium heat pipes (SAHP)". Applied Thermal Engineering, 52(2), pp.498-504.

Gorny, B., Niendorf, T., Lackmann, J., Thoene, M., Troester, T. and Maier, H.J., 2011. "In situ characterization of the deformation and failure behavior of non-stochastic porous structures processed by selective laser melting". Materials Science and Engineering: A, 528(27), pp.7962-7967.

Grin, Y. and Nesper, R., 2011. "Periodic Space Partitioners (PSP) and their relations to crystal chemistry". Zeitschrift für Kristallographie Crystalline Materials, 226(8), pp.692-710.

MathWorks, Inc, 1996. "MATLAB: Application program interface guide". Vol. 5. MathWorks.

Hibbett, Karlsson and Sorensen, 1998. "ABAQUS/standard: User's Manual". Vol. 1. Hibbitt, Karlsson & Sorensen.

Johnson, G.R., 1983. "A constitutive model and data for materials subjected to large strains, high strain rates, and high temperatures". Proc. 7th Inf. Sympo. Ballistics, pp.541-547.

Maskery, I., Aboulkhair, N.T., Aremu, A.O., Tuck, C.J. and Ashcroft, I.A., 2017. "Compressive failure modes and energy absorption in additively manufactured double gyroid lattices". Additive Manufacturing, 16, pp.24-29.

McKown, S., Shen, Y., Brookes, W.K., Sutcliffe, C.J., Cantwell, W.J., Langdon, G.S., Nurick, G.N. and Theobald, M.D., 2008. "The quasi-static and blast loading response of lattice structures. International Journal of Impact Engineering", 35(8), pp.795-810.

Mullen, L., Stamp, R.C., Brooks, W.K., Jones, E. and Sutcliffe, C.J., 2009. "Selective Laser Melting: A regular unit cell approach for the manufacture of porous, titanium, bone in‐growth constructs, suitable for orthopedic applications". Journal of Biomedical Materials Research Part B: Applied Biomaterials: An Official Journal of The Society for Biomaterials, The Japanese Society for Biomaterials, and The Australian Society for Biomaterials and the Korean Society for Biomaterials, 89(2), pp.325-334.

Murr, L.E., Gaytan, S.M., Medina, F., Martinez, E., Martinez, J.L., Hernandez, D.H., Machado, B.I., Ramirez, D.A. and Wicker, R.B., 2010. "Characterization of Ti–6Al–4V open cellular foams fabricated by additive manufacturing using electron beam melting. Materials Science and Engineering: A", 527(7-8), pp.1861-1868.

Qiu, C., Adkins, N.J. and Attallah, M.M., 2013. "Microstructure and tensile properties of selectively laser-melted and of HIPed laser-melted Ti–6Al–4V". Materials Science and Engineering: A, 578, pp.230-239.

Ramirez, D.A., Murr, L.E., Li, S.J., Tian, Y.X., Martinez, E., Martinez, J.L., Machado, B.I., Gaytan, S.M., Medina, F. and Wicker, R.B., 2011. "Open-cellular copper structures fabricated by additive manufacturing using electron beam melting". Materials Science and Engineering: A, 528(16-17), pp.5379-5386.

Schaedler, T.A. and Carter, W.B., 2016. "Architected cellular materials". Annual Review of Materials Research, 46, pp.187-210.

Scherer, M.R.J., 2013. "Gyroid and Gyroid-Like Surfaces". In Double-Gyroid-Structured Functional Materials (pp. 7-19). Springer, Heidelberg.

Schoen, A.H., 1970. "Infinite periodic minimal surfaces without self-intersections".

Valdevit, L., Jacobsen, A.J., Greer, J.R. and Carter, W.B., 2011. "Protocols for the Optimal Design of Multi‐Functional Cellular Structures: From Hypersonics to Micro‐Architected Materials". Journal of the American Ceramic Society, 94, pp.s15-s34.

Von Schnering, H.G. and Nesper, R., 1991. "Nodal surfaces of Fourier series: fundamental invariants of structured matter". Zeitschrift für Physik B Condensed Matter, 83(3), pp.407-412.

Thijs, L., Kempen, K., Kruth, J.P. and Van Humbeeck, J., 2013. "Fine-structured aluminium products with controllable texture by selective laser melting of pre-alloyed AlSi10Mg powder". Acta Materialia, 61(5), pp.1809-1819.

Yan, C., Hao, L., Hussein, A. and Raymont, D., 2012. "Evaluations of cellular lattice structures manufactured using selective laser melting". International Journal of Machine Tools and Manufacture, 62, pp.32-38.

Yan, C., Hao, L., Hussein, A., Young, P., Huang, J. and Zhu, W., 2015. "Microstructure and mechanical properties of aluminium alloy cellular lattice structures manufactured by direct metal laser sintering". Materials Science and Engineering: A, 628, pp.238-246.

Xiong, J., Mines, R., Ghosh, R., Vaziri, A., Ma, L., Ohrndorf, A., Christ, H.J. and Wu, L., 2015. "Advanced micro‐lattice materials". Advanced Engineering Materials, 17(9), pp.1253-1264.

RESPONSIBILITY NOTICE